Theoretical Studies of Mg(^{1}S, ^{3}P) Atom Reaction Mechanisms with HF, H_2O, NH_3, HCl, H_2S, and PH_3 Molecules#

Shogo SAKAI
Department of Information Systems Engineering, Faculty of Engineering, Osaka Sangyo University, Daito 574
(Received May 13, 1993)

The reaction mechanisms of Mg (^{1}S and ^{3}P) atom and XH molecules (X=F, OH, NH_2, Cl, SH, and PH_2) were studied by *ab initio* molecular orbital methods. A localized molecular orbital centroid analysis along the reaction coordinate shows that the Mg(^{1}S) atom insertion into the X–H bonds occurs through the pull-push mechanism. The activation barriers for the Mg(^{1}S) atom insertion are approximately the same values for each groups (X=F and Cl, OH and SH, and NH_2 and PH_2).

For the Mg(^{3}P) atom reactions with above six compounds, the hydrogen abstraction (produces MgH and H) and/or the exchange reaction (produces MgX and H) were studied. Both reactions of Mg(^{3}P) atom are the same one with two-step mechanism. The first step is an electron transfer from a Mg atom into the X–H bonds, which corresponds the transition state. The activation barrier height of the reaction is explained by adiabatic electron affinity of the X–H bonds. The second step is the formation of the products (Mg–X+H or Mg–H+X), which is clarified by the difference of Mg–X and Mg–H bond energies.

The reactions between metal atoms and small molecules have been a very active field for both experimental and theoretical studies during the past two decades. Especially the interaction of a main metal atom with a molecule is important for the understanding of the elemental reaction mechanisms of catalysis, surface chemistry, and the intermediate area between organic and inorganic chemistry. Many experimental studies of the reactions between a magnesium atom and alkyl halide molecules have been reported.[1] Most of them relate to the Grignard reagents. Ault[2] reported the formation and spectroscopic characterization of the unsolvated Grignard species H_3CMgX (X=Cl, Br, and I) by the matrix isolation technique. The insertion reaction occurred upon co-deposition of Mg and CH_3X at 15 K. Klabunde and co-workers[3] studied the reactivity of both main-group and transition-metal atoms under matrix isolation conditions and suggested the possibility that Mg metal clusters play an important role in the Grignard reaction. Breckenridge and Umemoto[4] observed, by the laser pump-and-probe technique, nascent internal energy distributions of MgH produced in the Mg(^{1}P) atom reaction with eleven molecules (CH_4, C_2H_6, neo-C_2H_{12}, CH_3NH_2, CH_3OH, $(CH_3)_2O$, $(CH_3)_4Si$, NH_3, PH_3, SiH_4, and GeH_4).

For the formation of the Grignard reagents, some theoretical studies were reported. Sakai and Jordan[5] presented the equilibrium geometry and associated vibrational frequencies of the H_3CMgCl species at the Hartree–Fock level. In a study relating the importance of magnesium clusters, structural and energetics calculations comparing a dimagnesium reagent (RMgMgX) with that of a simple one (RMgX), Jasien and Dykstra[6] showed that there is a 5—6 kcal mol^{-1} stabilization that arises from the formation of a dimagnesium reagent from a simple one for HF, CH_3F, and CH_3Cl. Davis[7] calculated the potential energy surfaces of Mg atom insertion into the carbon-halogen (F and Cl) bonds by the Hartree–Fock and Møller–Plessett perturbation methods. Chanquin and co-workers[8—10] studied the reactions of the excited Mg(^{1}P and ^{3}P) atom with H_2, HF, and CH_4 molecules by the SCF-CI, and the Møller–Plesset perturbation methods.

The systematic studies of an Al atom insertion reaction into X–H bonds (X=F, Cl, OH, SH, NH_2, and PH_2) were presented in my previous paper.[11] The Al insertion is a two-step mechanism; the first step is an electron transfer from an Al atom into the X–H antibonding orbital and the second is the formation of the Al–H bond. The transition state for the insertion closely relates to the first step. It is suggested that the energy barrier of the transition state can be estimated from the adiabatic electron affinity of the X–H bonds.

To investigate systematically the reaction mechanisms of an Mg atom with X–H compounds, I report the reaction mechanisms for twelve reactions of a Mg (^{1}S and ^{3}P) atom and HF, HCl, H_2O, H_2S, NH_3, and PH_3 molecules.

Theoretical Methods

Ab initio calculations were performed by use of the GAUSSIAN90[12] and GAMESS[13] programs. The standard 6-31G(d,p) basis set[14] was used at the unrestricted Hartree–Fock (UHF) level to determine the minima and transition states. Minima and transition states were verified by establishing that the matrixes of energy second derivatives[15] have zero and one negative eigenvalue, respectively. The reaction energies were determined at the HF-optimized structures by corrections of the fourth-order Møller–Plesset perturbation theory[16] with 6-311G(d,p)[17] or 6-311+G(d,p)[18] (included diffuse orbital) basis sets.

The reaction paths were calculated at the HF/6-31G-(d,p) level by determining the intrinsic reaction coordinate (IRC).[19] To interpret the results, a localized molecular orbital (LMO) centroid analysis[11,20] along the IRC was car-

#This paper is dedicated to the late Professor Hiroshi Kato.

ried out. The calculation of the localized orbitals was based on the Foster–Boys method.[21] For the open shell UHF calculation, the LMO's are determined independently for α and β electrons.

Results and Discussion

A. Mg (^{1}S) Insertion into X–H Bonds. The structural information and the HF/6-31G(d,p) total energy of each stationary point for the Mg (^{1}S) insertion into the X–H bonds (X=F, OH, NH_2, Cl, SH, and PH_2) are listed in Table 1.

HF and HCl: The Mg(^{1}S) atom insertion into the H–F or the H–Cl bond is the formation of the simplest Grignard reagent. The Mg atoms reactions with HF and HCl were studied previously,[6,7] and the transition state geometries have been located at the SCF, coupled cluster, and MP2 methods. The obtained geometry parameters here are similar to those of the previous reports. The Mg–F and the Mg–H bond lengths in the F(Mg)H transition state are 4.5 and 5.4% longer than those in the FMgH product, respectively. The Mg–Cl and the Mg–H bonds in the Cl(Mg)H transition state are 12.4 and 8.1% longer in length than those in the ClMgH product, respectively. From these results, the F(Mg)H transition state is a later transition state than the Cl(Mg)H transition state. Namely the transition state for the Mg insertion into the X–H bond (X=the second-row) is a later transition state than that of X=the first-row, except for the reaction of X=PH_2. For the Mg+HF reaction, the relative energies (the activation barrier and the heat of reaction) in Table 2 show the basis set dependency. At the MP4/6-31G(d,p) and the MP4/6-311G(d,p) calculations, the difference of the activation barriers is 6.4 kcal mol^{-1}, and that of the heat of reaction is 5.4 kcal mol^{-1}. On the other hand, for the Mg+HCl reaction, the difference of the activation barriers at both calculation levels is only 0.3 kcal mol^{-1}, and the heat of reactions are approximately equal. The basis set dependency for a molecule including fluorine atom is also found for the activation energy of the reaction Mg+CH_3F→CH_3MgF; the difference of the activation energies at the MP2/6-31G(d,p) and the MP2/D95(d,p) levels is 4.8 kcal mol^{-1}.

The activation energy including zero point corrections for the Mg+HF reaction is approximately equal to that for the Mg+Cl reaction; the difference is only 0.6 kcal mol^{-1}. The energy difference between the heat of reactions for the Mg+HF and the Mg+HCl reactions is 3.4 kcal mol^{-1}.

The centroids at the transition state geometries for both reactions are displayed in Fig. 1. The figure implied that the reactions are a pull–push mechanism; the lone pair electrons in X (X=F or Cl) move to the X–Mg bond region, and the electrons of Mg atom move to the Mg–H bond region. The variations of the Mg–H, the Mg–F, and the F–H bond distances along the IRC path for the Mg+HF reaction are shown in Fig. 2. The values of IRC ((AMU)$^{1/2}$ Bohr) indicate the reactant side for negative values and the product for positive values. Both curves of F–H and Mg–H bonds change drastically around the point −1.0 on the IRC path. Namely the exchange of the main elements (in the internal coordinates) for the reaction coordinate occurs at this point; from the Mg–H bond distance to the F–H bond distance.

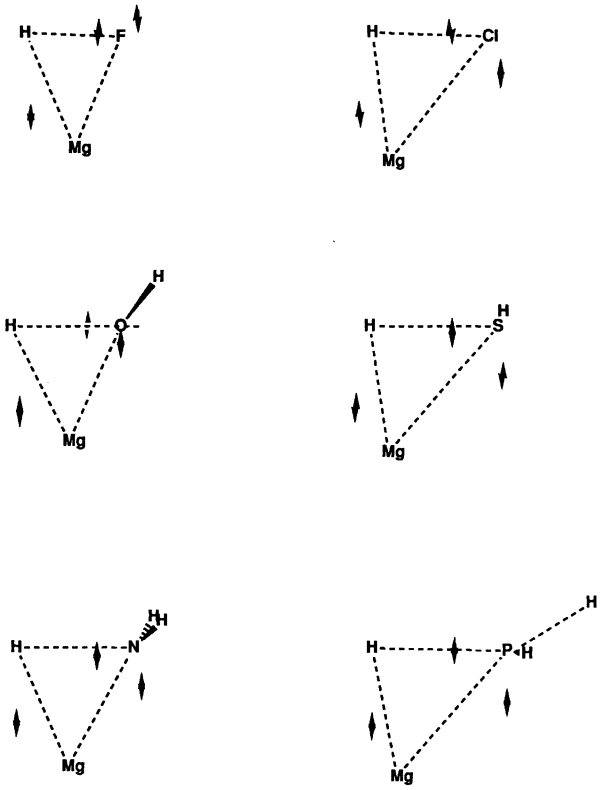

Fig. 1. Location of charge centroids of localized orbitals at the transition state for the Mg(^{1}S)+XH reactions. X=F, Cl, OH, SH, NH_2, and PH_2.

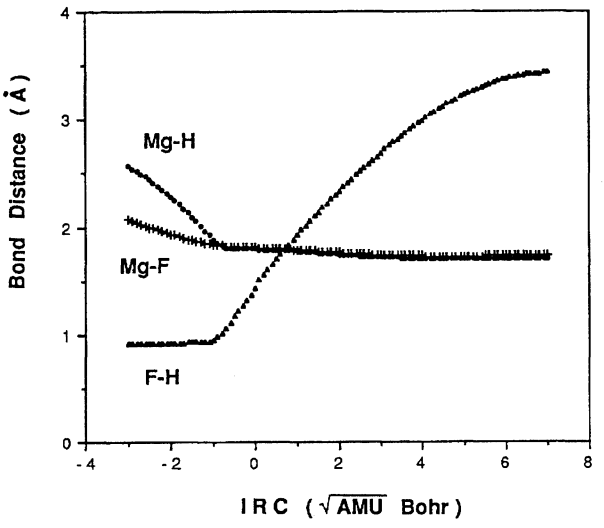

Fig. 2. Bond distances along the reaction path of the Mg(^{1}S)+HF reaction.

Table 1. The HF/6-31G(d,p) Energies and Structural Information of Stationary Points for Mg(^{1}S) Insertion into X–H Bonds

Structure	Point group	Bond Lengths, A			HF/6-31G(d,p)	Hessian
		Mg–X	Mg–H	X–H	hartree	Index[a]
F(Mg)H	C_s	1.808	1.792	1.437	−299.5244	1
FMgH	C_∞	1.730	1.700		−299.6612	0
HO(Mg)H	C_1	1.827	1.791	1.578	−275.5145	1
HOMgH	C_∞	1.754	1.706		−275.6415	0
Mg : NH_3	C_{3v}	2.672	1.014	3.298	−255.7868	0
H_2N(Mg)H	C_s	1.955	1.796	1.784	−255.6692	1
H_2NMgH	C_{2v}	1.894	1.711		−255.7855	0
Cl(Mg)H	C_s	2.485	1.831	1.766	−659.5840	1
ClMgH	C_∞	2.211	1.694		−659.7244	0
HS(Mg)H	C_1	2.493	1.824	1.949	−598.1756	1
HSMgH	C_s	2.317	1.702		−598.3017	0
H_2P(Mg)H	C_1	2.544	1.875	2.006	−541.9407	1
H_2PMgH	C_s	2.478	1.712		−542.0509	0

a) The number of negative eigenvalues of the matrix of energy second derivatives.

Table 2. Total and Relative Energies[a] for Stationary Points

Structure	MP4/6-31G(d,p)	MP4/6-311G(d,p)	E(vib)[b]	E(rel)[c]
Mg+HF	−299.8283	−299.9121	6.4	0.0 (0.0)
F(Mg)H	−299.7874	−299.8609	3.0	28.7 (22.3)
FMgH	−299.8868	−299.9619	4.5	−33.2 (−38.6)
Mg+H_2O	−275.8579	−275.9137	14.6	0.0 (0.0)
HO(Mg)H	−275.7935	−275.8488	10.1	36.3 (35.9)
HOMgH	−275.8820	−275.9381	11.1	−18.8 (−18.6)
Mg+NH_3	−256.0283	−256.0655	23.1	0.0 (0.0)
Mg : NH_3	−256.0315	−256.0681	24.3	−0.4 (−0.8)
H_2N(Mg)H	−255.9444	−255.9850	18.5	45.9 (48.0)
H_2NMgH	−256.0239	−256.0660	19.1	−5.6 (−1.3)
Mg+HCl	−659.8513	−659.9008	4.5	0.0 (0.0)
Cl(Mg)H	−659.8006	−659.8507	2.3	29.3 (29.6)
ClMgH	−659.9090	−659.9585	4.1	−36.6 (−36.6)
Mg+H_2S	−598.4611	−598.5088	10.2	0.0 (0.0)
HS(Mg)H	−598.3980	−598.4472	8.0	36.4 (37.4)
HSMgH	−598.4914	−598.5402	8.9	−21.0 (−20.3)
Mg+PH_3	−542.2333	−542.2792	16.2	0.0 (0.0)
H_2P(Mg)H	−542.1575	−542.2049	13.7	44.1 (45.0)
H_2PMgH	−542.2356	−542.2836	14.3	−4.7 (−3.3)

a) Total energies in hartrees and relative energies in kcal mol^{-1}. b) Vibrational energies in kcal mol^{-1}. c) Relative energies were obtained by MP4/6-311G(d,p) level. The values in parentheses were obtained by MP4/6-31G(d,p) level. Energies are included the zero point vibrational corrections.

The centroids along the IRC path for the Mg+HF insertion are illustrated in Fig. 3. The centroids (electrons) in the Mg atom part move to the Mg-H bond region at the range between points −1.0 and −0.5 on the IRC path. This motion of the centroids corresponds to the variations of the Mg–H and F–H bonds in Fig. 2. At the transition state, the centroids locate at almost the middle region of Mg and H atoms.

H_2O, H_2S, NH_3, and PH_3: As shown in the previous paper,[11] the largest stable complex in the adducts of an Al atom with the X–H compounds is Al : NH_3 of Al atom and ammonia, which have 11.7 kcal mol^{-1} in complexation energy at the MP4/6-31G (d,p) calculation level. The complexation energies of another adducts are smaller than that of Al : NH_3. The complexation energy of Mg : NH_3 is only 0.4 kcal mol^{-1}, and the stable complexes between Mg atom and another X–H compounds are not produced. Because the complexation energy between a main metal atom and a molecule including lone-pair-electrons is dominated[22] by two interaction energies; between the lone-pair-orbital and the lowest empty p orbital of the metal atom, and the lone-pair-orbital and the highest fully occupied s orbital of the metal atom. The former interaction is attractive, and the later is repulsive. The lowest empty p orbital energy level of Mg atom is 0.6 eV higher than that of Al

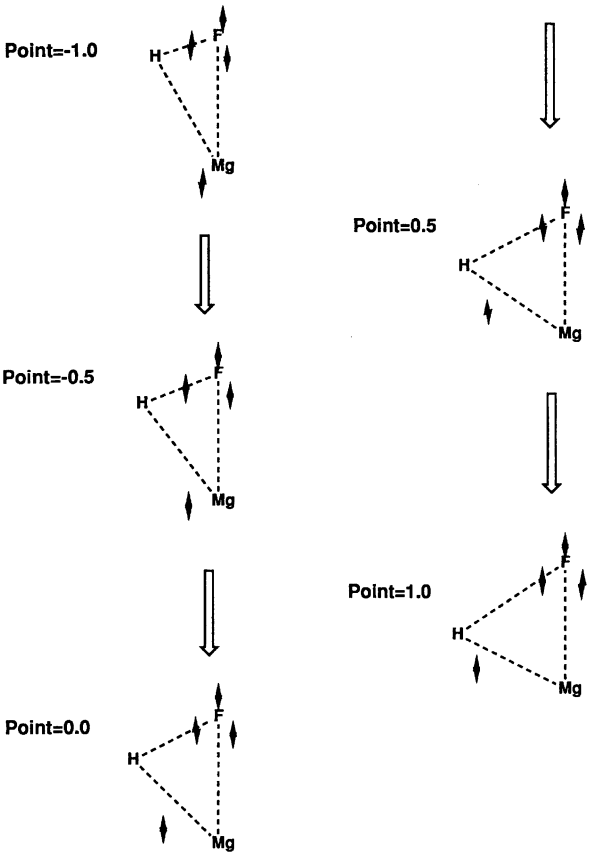

Fig. 3. Location of charge centroids of localized orbitals along the reaction path of the Mg(^{1}S)+HF reaction.

atom at the HF/6-31G(d) calculation. Therefore, it is considered that the complexation energy with Mg atom is smaller than that with Al atom.

The difference between the activation energies for the Mg+H_2O and the Mg+H_2S reactions is only 0.1 kcal mol^{-1}, and the difference between their heat of reactions is 2.2 kcal mol^{-1}. For the Mg+NH_3 and the Mg+PH_3 reactions, the difference of the activation energies is 1.8 kcal mol^{-1}, and of the heat of reactions is 0.9 kcal mol^{-1}. As above results, the activation energies for the Mg(^{1}S) insertion are approximately the same values for each groups (X=F and Cl, OH and SH, and NH_2 and PH_2).

The potential energies and the Mg–H, Mg–X, and X–H (X=O, S, N, and P) bond distances along the IRC paths for the Mg+H_2O, Mg+H_2S, Mg+NH_3, and Mg+PH_3 reactions are also calculated, and the feature is very similar to those of the Mg+HF and Mg+HCl systems.

The MgOH angle in HOMgH is 180 degree (linear), while the MgSH angle in HSMgH is 96.0 degree. The difference of both angles causes from their bond structures; the O–Mg bond has more ionic bonding ($HO^-\cdots MgH^+$) character than the S–Mg bond.

B. Mg (^{3}P)+X–H Reactions. The structural information and the HF/6-31G(d,p) total energy of each stationary point for the reactions of Mg(^{3}P) atom with X–H (X=F, OH, NH_3, Cl, SH, and PH_3) are listed in Table 3.

HF and HCl: For the Mg(^{3}P)+HX (X=F and Cl) reactions, two (^{3}A′ and ^{3}A″) states for the complexes (Mg : FH and Mg : ClH) exist. The Mg : FH complex at the ^{3}A′ state is 3.1 kcal mol^{-1} more stable in energy than that at the ^{3}A″ state at the MP4/6-311+G(d,p) calculation. In the Mg:ClH complex, the ^{3}A′ state is 2.6 kcal mol^{-1} more stable than the ^{3}A″ state. These four complexes are real complexes, which have no negative eigenvalue for their force constant matrixes. For the F (or Cl) abstraction, two transition states (^{3}A′ and ^{3}A″ states) were also obtained for both H(Mg)F and H(Mg)Cl systems. The energy barrier of the H(Mg)F transition state at the ^{3}A″ state is about 60 kcal mol^{-1} higher than that at the ^{3}A′ state at the MP4/6-31G(d, p) calculation; the energy barrier of the H(Mg)Cl transition state at the ^{3}A″ state is about 49 kcal mol^{-1} higher than that at the ^{3}A′ state. Though the both H(Mg)F and H(Mg)Cl transition states at the ^{3}A″ state have one negative eigenvalue for their force constant matrixes—the both transition state at the ^{3}A″ state are real transition states—these energy barriers are extremely high. Because the transition state at the ^{3}A″ state is the abstraction with the 3s radical orbital of Mg atom, and at the ^{3}A′ state is the abstraction with the $3p_\sigma$ radical orbital of Mg atom. Accordingly, we will discuss only the ^{3}A′ state below sections.

Both Mg(^{3}P)+HF and Mg(^{3}P)+HCl reactions have nonzero activation barriers at the HF calculation levels, and these barriers disappear at the MP levels. However, the obtained transition state geometries at the HF calculation are still useful, assuming the geometry variations along the reaction path at the HF calculation are approximately equal to those at the MP calculation.

The variations of the Mg–H, the Mg–F, and the F–H bond lengths along the IRC path for the Mg(^{3}P)+HF reaction are shown in Fig. 4. The values of IRC indicate the reactant side (complex Mg : FH) for negative values and the products side (MgF+H) for positive values. Both curves of F–H and Mg–H bonds change drastically at the point 0 (the transition state). The drastic variation for both bonds comes from the electron transfer at the transition state as the same as the reaction mechanism of the Al+XH insertion in the previous paper.[11] Namely an electron transfers from a metal atom to X–H antibonding orbital at the transition state. The LMO charge centroids at the transition state are displayed in Fig. 5. From the centroids, above reaction mechanism is also understood.

H_2O and H_2S: The ground states of the Mg(^{3}P) : OH_2 and the Mg(^{3}P) : SH_2 complexes are the $^3B_2$ and the ^{3}A″ states, respectively. The geometry of the Mg(^{3}P) : OH_2 complex has C_{2v} symmetry at the HF/6-31G(d,p) calculation. At the better calculation including electron correlation, the MP2/6-31G(d,p), the force

Table 3. HF/6-31G(d,p) Energy and Structural Information of Stationary Points for Reactions of Mg(^{3}P) Atom with XH Molecules

Structure	Point group	Bond lengths, Å			HF/6-31G(d,p)	Hessian
		Mg–X	Mg–H	X–H	hartree	Index[a]
Mg : FH	C_s	2.160		0.911	−299.5560	0
Mg(H)F	C_s	1.904	2.001	1.151	−299.5378	1
Mg : ClH	C_s	3.202		1.267	−659.5981	0
Mg(H)Cl	C_s	2.734	2.161	1.392	−659.5896	1
Mg : OH_2	C_s	2.114		0.945	−275.5804	0
Mg(H)OH	C_1	1.927	1.988	1.320	−275.5348	1
$MgSH_2$	C_s	2.790		1.327	−598.2139	0
Mg(H)SH	C_1	2.676	2.046	1.524	−598.1930	1
Mg : NH_3	C_s	2.247		1.003	−255.7572	0
Mg(H)NH_2	C_s	2.050	1.943	1.451	−255.6945	1
Mg : PH_3	C_s	2.745		1.398	−541.9973	0
Mg(H)PH_2	C_1	2.764	1.877	1.663	−541.9653	1

a) The number of negative eigenvalues of the matrix of energy second derivatives.

Table 4. Total and Relative Energies[a] for Stationary Points for Reaction of Mg(^{3}P) with X–H Molecules.

Structure	MP4/6-31G(d,p)	MP4/6-311+G(d,p)	E(vib)[b]	E(rel)[c]
Mg+HF	−299.7330	−299.8290	6.4	0.0 (0.0)
Mg : FH	−299.7556	−299.8403	7.2	−6.3 (−13.4)
Mg(H)F	−299.7519	−299.8372	2.2	−9.4 (−16.1)
MgF+H	−299.7817	−299.8632	1.1	−26.8 (−35.9)
Mg+H_2O	−275.7626	−275.8295	14.6	0.0 (0.0)
Mg : OH_2	−275.7955	−275.8557	15.9	−15.1 (−19.3)
Mg(H)OH	−275.7652	−275.8296	10.0	−4.7 (−6.2)
MgOH+H	−275.7756	−275.8402	7.8	−13.5 (15.0)
Mg+NH_3	−255.9330	−255.9770	23.1	0.0 (0.0)
Mg : NH_3	−255.9721	−256.0099	24.1	−19.7 (−23.5)
Mg(H)NH_2	−255.9205	−255.9656	18.5	2.6 (3.2)
MgH+NH_2	−255.8976	−255.9401	15.0	13.8 (14.1)
$MgNH_2$+H	−255.9169	−255.9637	15.6	0.9 (2.6)
Mg+HCl	−659.7560	−659.8067	4.5	0.0 (0.0)
Mg : ClH	−659.7622	−659.8128	5.0	−3.3 (−3.4)
Mg(H)Cl	−659.7645	−659.8165	2.0	−8.6 (−7.8)
MgCl+H	−659.8037	−659.8517	0.7	−32.1 (−33.7)
Mg+H_2S	−598.3658	−598.4150	10.2	0.0 (0.0)
Mg : SH_2	−598.3834	−598.4322	11.5	−9.5 (−9.7)
Mg(H)SH	−598.3737	−598.4248	7.8	−8.6 (−7.4)
MgSH+H	−598.3861	−598.4336	5.4	−16.5 (−17.6)
Mg+PH_3	−542.1380	−542.1851	16.2	0.0 (0.0)
Mg : PH_3	−542.1610	−542.2074	17.4	−12.8 (−13.2)
Mg(H)PH_2	−542.1398	−542.1891	13.8	−4.9 (−3.6)
MgH+PH_2	−542.1458	−542.1938	11.3	−10.4 (−9.8)
$MgPH_2$+H	−542.1315	−542.1774	10.8	−0.6 (−1.3)

a) Total energies in hartrees and relative energies in kcal mol^{-1}. b) Vibrational energies in kcal mol^{-1}. c) Relative energies were obtained by MP4/6-311G(d,p) level. The values in parentheses were obtained by MP4/6-31(d,p) level. Energies are included the zero point vibartional corrections.

constant matrix at the C_{2v} geometry has one negative eigenvalue for out-of-plane (Table 4). However, the negative eigenvalue is only 60 cm^{-1} and the energy difference between the C_{2v} and C_s optimized geometries is only 0.002 kcal mol^{-1} at the MP2/6-31G(d,p) calculation. The potential energy curve along the IRC path for the Mg(^{3}P)+H_2S reaction is displayed in Fig. 6. This potential curve is different from those of the other three reactions, Mg(^{3}P) with HF, HCl, and H_2O, which includes a shoulder in it. Such shoulder also can be found in the IRC potential curves for Al (^{2}P)+XH insertion reactions. The potential curve with a shoulder suggests that the reaction includes two or more elementary mechanisms. The variations of the Mg–H, the Mg–S, and the S–H bond lengths along the IRC path for the Mg(^{3}P)+H_2S reaction are illustrated in Fig. 7. From

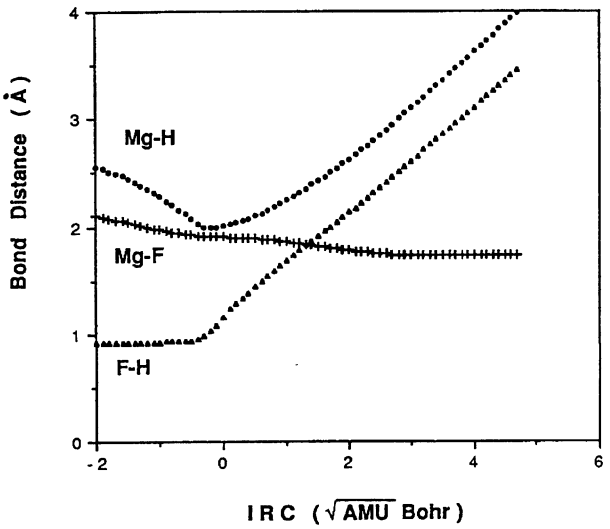

Fig. 4. Bond distances along the reaction path of the $Mg(^3P)$+HF reaction.

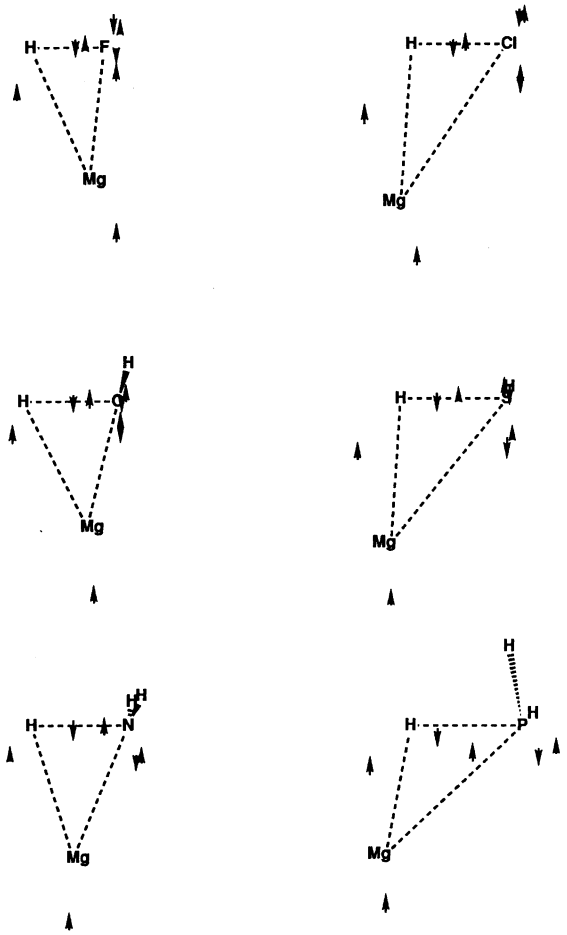

Fig. 5. Location of charge centroids of localized orbitals at the transiton state for the $Mg(^3P)$+XH reactions. X=F, Cl, OH, SH, NH_2, and PH_2.

the figure, two mechanisms producing MgH+SH and MgSH+H are included on the reaction path. The first process looks like MgH+SH until around the range between points 1.0 and 2.0 on the IRC path; the second looks like MgSH+H. The final products of the reaction are MgSH+H because of the difference of the heat of reactions; -0.5 kcal mol^{-1} for MgH+SH and -11.1 kcal mol^{-1} for MgSH+H at the HF/6-31 G(d,p) level. For the reaction $Mg(^3P)$+H_2O, the potential curve has no shoulder. Because the transition state (H(Mg)OH) is 6.3 kcal mol^{-1} in energy below the products MgH+OH.

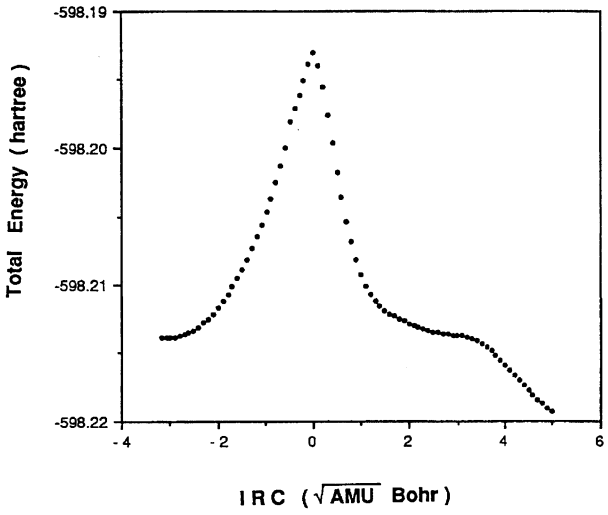

Fig. 6. Total energy along the reaction path of the $Mg(^3P)$+H_2S reaction.

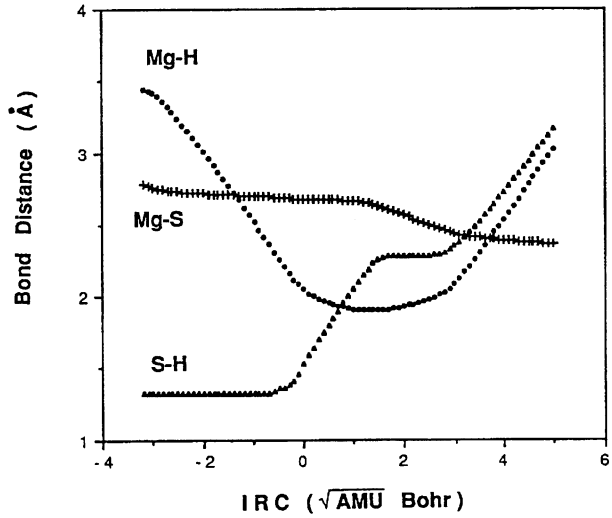

Fig. 7. Bond distances along the reaction path of the $Mg(^3P)$+H_2S reaction.

NH_3 and PH_3: In the Mg:NH_3 and Mg:PH_3 complexes, I assumed C_s symmetry for the HF-geometry-optimization calculation. Two states ($^3A'$ and $^3A''$) for both complexes were obtained. The force constant matrixes at the $^3A'$ states for both complexes have one negative eigenvalue (out-of-plane) for each, and at the $^3A''$ states have no negative eigenvalue. The energy differences between the $^3A'$ state and the $^3A''$ state for each Mg:NH_3 and the Mg:PH_3 complexes are 0.0008

kcal mol^{-1} and 0.09 kcal mol^{-1} at the HF/6-31(d,p) calculations, respectively.

At the transition state of the Mg(^{3}P)+NH_3 reaction, the IRC path obtained at the HF/6-31G(d,p) level relates to the Mg : NH_3 complex for the reactant side and a complex between MgH and NH_2 species for the products side. The MgH$\cdots$$NH_2$ complex is about 15 kcal mol^{-1} stable measured from the isolated MgH and NH_2 at the MP4/6-31G(d,p) level. The $MgNH_2$+H products are about 1.6 kcal mol^{-1} more stable in energy than the MgH+NH_2 products at the HF/6-31G(d,p) level. On the other hand, the IRC path obtained at the MP2/6-31G(d,p) level relates to the Mg : NH_3 complex and a complex between $MgNH_2$ and H species. The complex $MgNH_2\cdots$H is about 5 kcal mol^{-1} stable measured from the isolated $MgNH_2$ and H at the MP4/6-31G(d,p) level. The $MgNH_2$+H products are about 19 kcal mol^{-1} more stable in energy than the MgH+NH_2 product at the MP2/6-31G(d,p) level. Thus the products along the IRC path are different by the calculation levels. The bond energies of the Mg–X (X=F, Cl, OH, SH, NH_2, PH_2, and H) at the HF and the MP calculation levels are listed in Table 5. From the table, it is found that the reaction products are understood from the energy difference of the Mg–X bond and the Mg–H bond. Namely the transition state is dominated by the electron transfer, while the products are dominated by the bond energy.

The obtained transition state of the Mg(^{3}P)+PH_3 system correlates to both the complex Mg : PH_3 and a weak complex of MgH and PH_2. The complexation energy of the weak complex, HMg$\cdots$$PH_2$, is 3.1 kcal mol^{-1} at the MP4/6-31G(d,p) calculation. From the energy difference of the Mg–H and the Mg–PH_2 bonds, the reaction probability produced $MgPH_2$+H is lower than that produced MgH+PH_2.

Conclusions

The reaction mechanisms of Mg (^{1}S, and ^{3}P) atoms and the X–H (X=F, Cl, OH, SH, NH_2, and PH_2) molecules were studied by the *ab initio* molecular orbital methods. In the Mg(^{1}S) insertion into the X–H bonds, the reaction is the pull–push mechanism; the lone pair electrons in the X part move to the X–Mg bond region, and the electrons in Mg atom move to the Mg–H bond region. The above second process corresponds to the transition state (the activation energy barrier).

The Mg(^{3}P) atom reactions with X–H molecules are a two-step mechanism. The first step is the electron transfer from the metal atom to the X–H bond, and this process corresponds to the transition state (the activation energy barrier). From the results, I suggest that the activation energies are related to the adiabatic electron affinity of the X–H bonds. The adiabatic electron affinities[11] of the X–H bonds are 59.7, 83.0, 104.0, 26.5, 47.7, and 59.1 kcal mol^{-1} for the H–F, H–OH, H–NH_2, H–Cl, H–SH, and H-PH_2 bonds, respectively. The trend in barrier height relates with the values of the calculated adiabatic electron affinity in the first- and second-row atoms separately. This is the same to the previous conclusion[11] as the reaction Al+XH. The second step is the formation of the products. Whether the hydrogen abstraction (Mg–H+X) by the metal or the exchange reaction (Mg–X+H) is determined by the energy difference of the Mg–X and Hg–H bonds.

Table 5. Bond Energy by HF and MP Calculations (kcal mol^{-1})

Bond	HF/6-31G(d,p)	MP4/6-31G(d,p)
Mg—F	−74.7	−98.8
Mg—Cl	−65.0	−67.9
Mg—OH	−49.4	−64.5
Mg—SH	−37.3	−41.7
Mg—NH_2	−28.4	−38.8
Mg—PH_2	−14.4	−17.7
Mg—H	−26.8	−26.7

This research was supported by a Grant-in-Aid for Scientific Research on Priority Areas "Theory of Chemical Reactions" from the Ministry of Education, Science and Culture, for which I express my gratitude. The numerical calculations were carried out at the Computer Center of the Institute for Molecular Science (IMS) and Osaka Sangyo University (CONVEX C240 minisupercomputer).

References

1) W. E. Lindsell, "Comprehensive Organometallic Chemistry," ed by G. Wilkinson, Pergamon Press, Oxford (1982), Vol. 1.
2) B. S. Ault, *J. Am. Chem. Soc.*, **102**, 3480 (1980).
3) Y. Tanaka, S. C. Davis, and K. J. Klabunde, *J. Am. Chem. Soc.*, **104**, 1013 (1982).
4) W. H. Breckenridge and H. Umemoto, *J. Chem. Phys.*, **81**, 3852 (1984).
5) S. Sakai and K. D. Jordan, *J. Am. Chem. Soc.*, **104**, 4019 (1982).
6) P. G. Jasien and C. E. Dykstra, *J. Am. Chem. Soc.*, **105**, 2089 (1983); P. G. Jasien and C. E. Dykstra, *Chem. Phys. Lett.*, **106**, 276 (1984); P. G. Jasien and C. E. Dykstra, *J. Am. Chem. Soc.*, **107**, 1891 (1985).
7) S. R. Davis, *J. Am. Chem. Soc.*, **113**, 4145 (1991).
8) P. Chaquin, A. Sevin, and H. Yu, *J. Phys. Chem.*, **89**, 2813 (1985).
9) P. Chaquin, *J. Phys. Chem.*, **91**, 1440 (1987).
10) P. Chaquin, A. Papakondylis, C. Giessner-Prettre, and A. Sevin, *J. Phys. Chem.*, **94**, 7352 (1990).
11) S. Sakai, *J. Phys. Chem.*, **96**, 8369 (1992).
12) M. J. Frisch, M. Head-Gordon, G. W. Trucks, J. B. Foresman, H. B. Schlegel, K. Raghavachari, M. A. Robb, J. S. Binkley, C. Gonzalez, D. J. Defrees, D. J. Fox, R. A. Whiteside, R. Seeger, C. F. Melius, J. Baker, R. L. Martin, L. R. Kahn, J. J. P. Stewart, S. Topiol, and J. A. Pople,

"Gaussian90," Gaussian, Inc., Pittsburgh, PA (1990).
13) M. Dupuis, D. Spangler, J. J. Wendoloski, "NRCC Software Catalog 1980," Vol. 1, program QG01; M. W. Schmidt, K. K. Baldridge, J. A. Boatz, J. H. Jensen, S. Koseki, M. S. Gordon, K. A. Nguyen, J. L. Windus, and S. T. Llbert, *QCPE Bull.*, **10**, 52 (1990).
14) P. C. Hariharan and J. A. Pople, *Mol. Phys.*, **27**, 209 (1974); M. M. Francl, W. J. Pietro, W. J. Hehre, J. S. Binkley, M. S. Gordon, D. J. DeFrees, and J. A. Pople, *J. Chem. Phys.*, **77**, 3654 (1982).
15) J. A. Pople, J. S. Binkley, and R. Seeger, *Int. J. Quantum Chem.*, **9**, 229 (1975); J. A. Pople, R. Krishnan, H. B. Schegel, and J. S. Binkley, *Int. J. Quantum Chem.*, **S13**, 225 (1979).
16) C. Møller and M. S. Plesset, *Phys. Rev.*, **46**, 618 (1934); J. S. Binkley and J. A. Pople, *Int. J. Quantum Chem.*, **9**, 229 (1975); J. A. Pople, J. S. Binkley, and R. Seeger, *Int. J. Quantum Chem.*, **S10**, 1 (1976); R. Krishnan and J. A. Pople, *Int. J. Quantum Chem.*, **14**, 91 (1978); R. Krishnan, M. J. Frisch, and J. A. Pople, *J. Chem. Phys.*, **72**, 4244 (1980).
17) A. D. McLean and G. S. Chandler, *J. Chem. Phys.*, **72**, 5639 (1980); M. J. Frisch, J. A. Pople, and J. S. Binkley, *J. Chem. Phys.*, **80**, 3261 (1984).
18) T. Clark, J. Chandrasekhar, G. W. Spitznagel, and G. P. V. R. Schleyer, *J. Comput. Chem.*, **4**, 294 (1983).
19) K. Fukui, *J. Phys. Chem.*, **74**, 4161 (1970); K. Ishida, K. Morokuma, and A. Komornicki, *J. Chem. Phys.*, **66**, 2153 (1977).
20) S. Sakai and K. Morokuma, *J. Phys. Chem.*, **91**, 3661 (1987); S. Sakai, J. Deisz, and M. S. Gordon, *J. Phys. Chem.*, **93**, 1888 (1989); S. Sakai, *J. Phys. Chem.*, **95**, 175 and 7089 (1991); S. Sakai and M. Nakamura, *J. Phys. Chem.*, **97**, 4960 (1993).
21) J. M. Foster and S. F. Boys, *Rev. Mod. Phys.*, **32**, 296 and 300 (1960).
22) S. Sakai and S. Inagaki, *J. Am. Chem. Soc.*, **112**, 7961 (1990).